Synthetic Fiber Capstan Drives For Highly Efficient, Torque Controlled, Robotic Applications

Anirban Mazumdar, Steven J. Spencer, Clinton Hobart, Jeffrey Dabling, Timothy Blada, Kevin Dullea, Michael Kuehl and Stephen P. Buerger

Abstract—This paper describes the design and performance of a synthetic rope on sheave drive system. This system uses synthetic ropes instead of steel cables to achieve low weight and a compact form factor. We demonstrate how this system is capable of 28Hz torque control bandwidth, 95% efficiency, and quiet operation, making it ideal for use on legged robots and other dynamic, physically interactive systems. Component geometry and tailored maintenance procedures are used to achieve high endurance. Endurance tests based on walking data predict that the ropes will survive roughly 247,000 cycles when used on large (90kg), fully actuated bipedal robot systems. The drive systems have been incorporated into two novel bipedal robots capable of 3D unsupported walking. Robot data illustrates effective torque tracking and nearly silent operation. Finally, comparisons with alternative transmission designs illustrate the size, weight, and endurance advantages of using this type of synthetic rope drive

Index Terms—Mechanism Design of Mobile Robots, Humanoid Robots, Humanoid and Bipedal Locomotion.

I. INTRODUCTION

E LECTROMAGNETIC motors are widely used in robot applications due to their high peak efficiency, power density, quiet operation, and commercial availability. However, their low torque density frequently necessitates speed reduction mechanisms [1]. Such mechanisms can reduce efficiency, lower bandwidth, and add substantial weight and complexity [2].

Cable-based mechanisms can provide speed reduction with reduced weight and enhanced design flexibility when compared with conventional gearing. Cable-based drive systems are used for robot arms, walking robots, and haptic interfaces [3]–[5]. Capstan drives employ dual cables wrapped in a figure-eight shape around the input (sheave) and the output (pulley). These drives offer low inertia, zero backlash, and high stiffness [6], [7]— all of which are advantageous for high-quality impedance control.

Manuscript received: August, 31, 2016; Revised November, 24, 2016; Accepted December, 8, 2016.

This paper was recommended for publication by Editor Paolo Rocco upon evaluation of the Associate Editor and Reviewers' comments. *This work was supported as part of DARPA's Maximum Mobility and Manipulation (M3) Program

A. Mazumdar, S. Spencer, C. Hobart, J. Dabling, T. Blada, K. Dullea, M. Kuehl, and S. Buerger are with High Consequence Automation and Robotics, Sandia National Laboratories, Albuquerque, NM, USA. amazumd@sandia.gov; sbuerge@sandia.gov

Sandia National Laboratories is a multi-mission laboratory managed and operated by Sandia Corporation, a wholly owned subsidiary of Lockheed Martin Corporation, for the U.S. Department of Energy's National Nuclear Security Administration under contract DE-AC04-94AL85000.

Digital Object Identifier (DOI): see top of this page.

Steel cables for such drives provide zero cold creep, and if designed properly, can survive hundreds of thousands of cycles [8]. However, steel cables require a large ratio of minimum bend radius to cable radius—typically 18:1 in the 3mm diameter range [9]. This results in large system components.

A. Approach: Synthetic Rope Drives

Synthetic ropes offer potential performance improvements over steel cables. Synthetic ropes such as Vectran can have higher strength to weight ratios than steel [10]. In addition, synthetic ropes can wrap around pulleys with an 8:1 diameter ratio [11]. At diameter ratios around 8:1, Vectran is expected to maintain $\sim 85\%$ of its tensile strength [12]. This enables components that are roughly 65% smaller than their steel cable counterparts. This ability of synthetic drives to provide high torque density is especially appealing for mobile robots [13]. Synthetic ropes have been used for a variety of robotic applications including tendon drives and Bowden cable systems in robotic manipulators, automated test-beds, and efficient quadruped robots [13]–[15].





Fig. 1. A rendering of the capstan drive and a photograph of the capstan drive implemented on one of Sandia's bipedal robots.

However, there are several drawbacks with synthetic ropes. In spite of their high strength, cycle life can be extremely brief (hundreds to a few thousand cycles). The primary failure mode is believed to be material breakdown caused by abrasion between rope fibers [16]. Maintaining tension throughout use is critical both to achieve high stiffness and maximize cycle life. Keeping proper tension is complicated by the fact that some common rope types cold creep under load. Also, the end terminations are frequently weaker than the rope and can limit performance if not carefully designed and protected. Due to these factors, the cycle life of synthetic ropes is difficult to model and can be impractically brief.

Our team has developed a new drive system for bipedal walking robots that addresses each of the aforementioned issues and has demonstrated success in practice. This system, shown in Fig. 1, uses braided Vectran (spun liquid crystal polymer) rope which does not cold creep [10]. The use of braided rope (as opposed to twisted or plaited) reduces the size of the recommended sheave [11]. A custom sheave and pulley design supports the rope shape under load, prevents rubbing between successive turns of the rope, and ensures that the rope rides only on highly polished surfaces. A compact tensioning system enables simple installation, replacement, and tightening of the ropes. Small rope terminations have been developed and are capable of handling high loads. These terminations are further protected through geometry to reduce loading at the rope ends.

The system performance: fatigue life of > 200,000 cycles, 95% efficiency across relevant load and speed conditions, 28Hz torque control bandwidth, and virtually silent operation are all competitive with state of the art drive systems and meet the needs of dynamically-controlled legged robots.

Our low reduction Vectran drive system compares favorably with more traditional alternatives. The reduction ratios (10:1 and lower) described in this work push the limits of harmonic drives due to the need for low tooth count and large flex spline deformations. The synthetic rope drive system offers mass savings and reduced backlash when compared with traditional gearing, and provides size savings over synchronous belt drives. Finally, when compared with steel cable drives (the most similar alternative), our Vectran rope drive demonstrates dramatically better endurance life. The main disadvantages of our approach are the limited range of output motion ($\sim 270^{\circ}$), the finite endurance life of the ropes, and the need to monitor rope tension and overall condition.

B. Paper Overview

In this paper we introduce the properties of drive systems for impedance controlled legged robots, and then describe how our synthetic rope drive is well suited for such applications. The results of bench tests to characterize strength, bandwidth, and efficiency are summarized. Rope endurance results from a bench-level dynamometer are presented, and best practices for maximizing endurance are identified. The rope drive is compared with several alternative transmission approaches such as gearing, harmonic drives, belts, and steel cables. We conclude with the incorporation of our rope drives into 3D, fully actuated bipedal robots.

II. DRIVE SYSTEMS FOR IMPEDANCE CONTROLLED LEGGED ROBOTS

Drive systems for legged robots require high efficiency, high bandwidth, minimal backlash, high specific torque and torque density, and variable impedance. The need for variable, controlled impedance is critical for systems that interact dynamically with the environment. Dynamic walking requires low and compliant leg impedance during transitions into and out of ground contact in order to limit force spikes in response to perturbations (e.g. due to uncertainty in the ground

surface). Higher impedance is required to control the leg trajectory during swing and to maintain posture under load. Stiff but intrinsically low impedance drive systems that allow the implementation of techniques like "simple" impedance control [17] are preferred. Such systems can implement a wide range of output impedance using exclusively motion feedback [18], which makes them largely invulnerable to the contact instability challenges introduced by torque feedback [19]. It is also noteworthy that when torque feedback is used to overcome high intrinsic impedance, energy must be expended to overcome internal friction and inertia, thereby reducing efficiency. Since motor friction and inertia are reflected to the output with the square of the transmission ratio, low gear ratios are needed to achieve intrinsically low impedance [20].

Our examination of existing technologies did not provide a suitable option that achieved our desired combination of efficiency, bandwidth, torque density, zero backlash, and low intrinsic impedance. Therefore we developed a new drive system that better meets the application needs. We believe this system is broadly applicable to legged robots and other dynamic, physically interactive systems. The system outlined in this paper has demonstrated the following properties which enable it to provide effective, versatile, highly efficient walking control via simple impedance control.

- Single-stage speed reductions ranging from 5:1 to 10:1.
 These ratios were identified using a combination of analysis and optimization which seek to minimize motor energy consumption and ensure that reflected motor inertia and friction do not dominate the output dynamics.
- 2) Output torque capability of 150Nm 200Nm (depending on gear ratio) and speed capability of up to 15rad/s. These metrics are based on walking simulations and provide sufficient capability for a 90kg humanoid biped robot walking at a range of speeds.
- 3) Accurate torque control without torque feedback. Since transmission friction, backlash, and inertia are minimized, closed loop current control of the motor can be used to control output joint torque. This eliminates the need for torque sensing at each joint and removes losses associated with overcoming internal impedance.
- 4) Torque control bandwidth of 28Hz. This is comparable with existing electromagnetic torque control systems such as motor driven series elastic actuators [21] and achieves high fidelity control during bipedal walking experiments.
- 5) Efficiencies of 95%. This is comparable to existing high performance systems such as low ratio, single stage, spur and planetary gearboxes [22], [23].
- 6) Demonstrated endurance of 240,000+ cycles. This corresponds to more than 190 hours of use.
- Very low sound levels, enabling quiet operation and allowing human workers to communicate and work safely around robotic systems.

III. CAPSTAN DRIVE SYSTEM DESIGN

A. Sheave and Pulley Design

The capstan drive architecture uses two cylindrical devices. The small diameter "sheave" is attached to the output of

3

the motor, while the larger diameter "pulley" is connected to the joint output. Two identical ropes are wrapped around the sheave and pulley to carry loads in both directions. In the following sub-sections we describe 4 key features of our design that are essential to overcoming the unique challenges of synthetic ropes.

- 1) Sheave and Pulley Properties: A helical contour is machined into the sheave in order to prevent the rope from wrapping and rubbing on itself. The helix is carefully designed to capture the rope and prevent it from flattening. This feature is visible in Fig. 1. In order to prevent abrasion between the surface and the rope, both the sheave and pulley are machined to a very high polish.
- 2) Rapid Rope Tensioning: Maintaining rope tension is essential for maximizing rope life and eliminating backlash. If a proper pre-load is not maintained, the ropes can go slack. This can result in shock loads to the rope which we found to dramatically reduce rope life (Section VII).

The ropes are installed loose and then tensioned before use. A wear-in period of roughly 10-50 cycles is required, allowing the ropes to settle into the pulley and sheave and distribute the preload evenly. Tensioning is repeated following the wear-in period and occasionally thereafter. Generally, we found that after 1000 cycles, additional tensioning is unnecessary. Our rope tensioning system uses a tensioning pulley mounted on a carriage. As the bolt is tightened, the tensioning pulley and trolley carriage move, stretching the rope. This approach enables rapid tensioning at any joint whenever it is required.

3) Termination Protection: Since the terminations are generally weaker than the rope itself (Section IV), they are protected using extra wraps on both the sheave and pulley. The rope tension, T_r , consists of two components: the preload tension, T_{pre} , and the tension from the joint torque, T_{torque} . The preload tension is used to prevent the rope from going slack and is uniformly distributed along the rope and terminations. However, the capstan effect significantly reduces the force from the joint torque that is felt by the termination. The coefficient of static friction between Vectran cable and aluminum, μ , was measured to be 0.3. The angle of engagement, ψ , is $\geq 2\pi$ for the sheave, and π for the pulley. The force on the termination, F_{term} , can be determined using the following expression

$$F_{term} = \frac{T_{torque}}{e^{\mu\psi}} + T_{pre} \tag{1}$$

Alternative rope fixation methods such as calking, or sewing have demonstrated the ability to get up to 85-90% of the rope strength [24].

4) Rope Lubrication: Lubrication can reduce abrasive wear between adjacent rope fibers and against the aluminum surfaces, improving efficiency (Section VI) and increasing cycle life by approximately 20% (Section VII). We use Krytox grease to lubricate the ropes. Since the lubricant reduces the friction between the aluminum and the rope, it also reduces the capstan effect. Therefore, we do not apply lubricant to the extra wraps on the sheave or pulley.

B. Rope Selection

Examples of synthetic ropes include high modulus polyethylene (Dyneema), para-aramid fiber (Kevlar), poly-p-phenylene-2, 6-benzobisoxazole (Zylon/PBO), and spun liquid crystal polymer (Vectran). All of these fiber types provide excellent strength to weight ratios. Of these, Vectran provides the best combination of very low cold creep and relatively low sensitivity to UV/visible light (depending on coating) [8], [12].

The rope diameter impacts pulley/sheave geometry as well as the load capacity and stiffness. We estimate the tension in the rope, T_r , using the output torque, τ_J , the transmission ratio, N, and the diameter of the rope d_r .

Using the manufacturer's minimum diameter ratio of 8:1, the sheave diameter, D_s , is

$$D_s = 8d_r \tag{2}$$

The pulley diameter, D_p , can then be determined using the transmission ratio, and the tension in the rope can be calculated using the desired torque, τ_J , and the preload tension, T_{pre} .

$$D_p = ND_s \tag{3}$$

$$T_{torque} = \frac{2\tau_J}{D_p} \tag{4}$$

$$T_r = T_{torque} + T_{pre} = \frac{2\tau_J}{8Nd_R} + T_{pre} \tag{5}$$

We present an example design using a transmission ratio of N=6 and a desired joint torque of 150Nm. These numbers are based on loading at the knee joint of our robots and represent worst-case torque conditions from initial simulations. Based on the expected loading we selected New England Ropes' 3mm diameter, V12 12-stranded Vectran rope (break strength of 9400N, linear density of 7.4g/m). This rope comes treated with the company's Marine-Tech coating for improved abrasion and UV resistance. In order to ensure that the rope does not go slack, we treat T_{pre} as equal to the max joint torque, τ_J . Under these conditions, the peak rope tension was estimated to be 3950N, or 42% of the break strength. The same rope was used for all the leg joints; many joints see lower loads than the knee, resulting in lower load percentage.

C. Rope Termination

Ropes were terminated using stainless steel cylinders with tapered holes as shown in Fig. 2. The cylinder is placed over the rope end and the rope is then prepared by spreading out the individual fibers. The tapered hole is filled with epoxy, forming an epoxy wedge that resists rope movement. One drawback to this method is that the epoxy can wick up the rope. This means that the rope must depart straight from the termination.

IV. ROPE CHARACTERIZATION

The static properties of the terminated 3mm diameter Vectran cable were measured using an MTS servo-hydraulic load frame (Model 312.21) with 97860N load capacity. Rope samples of 305mm in length were pulled to moderate loads, cycled, and pulled until failure. A set of 9 samples were



Fig. 2. CAD illustrations and photographs of the rope terminations.

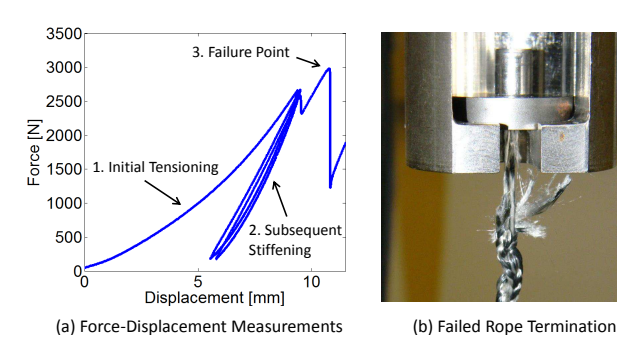


Fig. 3. Force-displacement data from rope pull testing (a), and a photograph of a failed rope termination (b).

tested to failure. Every sample failed at the termination. The average force at failure was 4300N, and the worst performing termination failed at 2982N.

Data from the worst-case pull test is shown in Fig. 3. The data in Fig. 3-a shows 3 regimes. Regime 1 is the initial tensioning of the rope, causing it to straighten and settle. Relaxing the force to nearly zero still leaves a 5mm change in length, indicating permanent elongation. Regime 2 is the cyclic loading of the rope between 180N and 2700N. This behavior is approximately linear with minor hysteresis. The stiffness in this second regime ($\sim 618kN/m$) is higher than during the initial loading ($\sim 287kN/m$). When used with the sheave and pulley, the rope stiffness depends on the active length of the rope. Finally, regime 3 represents the failure of the rope at 2982N at the termination. A close up view of a failed termination is shown in Fig. 3-b.

The weakest termination failed in tensile testing at 2982N or 32% of the rope's tensile strength. While this minimum termination failure force is below the maximum estimated tensile load (3950N), the capstan effect at the pulley and bobbin ensures that the termination sees a reduced load. The worst case maximum tensile load on the termination is 2736N which is 240N less than the failure load for the worst performing termination, and 1564N less than the average termination failure load. Therefore, this termination design is sufficient for our requirements.

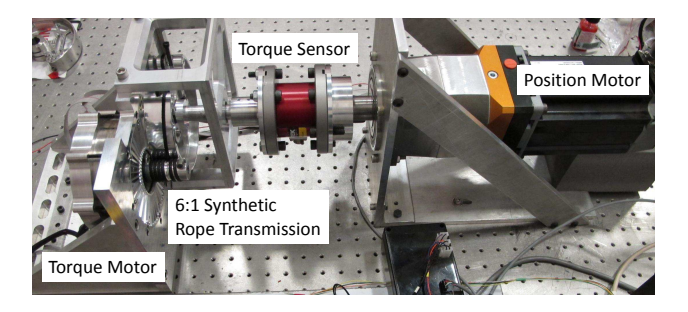


Fig. 4. A photograph of the dynamometer designed for high torque and high speed testing.

V. DYNAMIC RESPONSE

A. Experimental Test-bed

A bench-level system (Fig. 4) was developed to evaluate the performance of the synthetic rope transmission. This testbed is based around an Allied Motion Megaflux (MF0127032-X0X) motor connected to a 6:1 Vectran rope capstan drive. The Megaflux motor is operated in torque control mode (closed loop current control) and is referred to as the "torque motor." The torque motor is identical to the hip flexion motors on one of our robots [25], and is very similar to many of the other robot joint motors. The torque motor is controlled using an Allied Motion XDA-16000000 motor drive.

The torque motor shaft is connected through a Futek FSH00682 torque sensor to the shaft of the "position motor," a Parker Hannifin DC motor with a 25:1 gear reduction (MPP1154B70). The position motor is controlled in position control mode using an ACS CMhp1C0E1N4004 controller. The position motor imposes a motion trajectory on the torque motor while the torque motor provides a corresponding torque profile. This configuration is used to evaluate the performance of the rope drive and other components under simulated bipedal walking conditions.

B. Frequency Response

Torque control frequency response experiments were performed with the output of the position motor regulating to zero. The input to the system was the current commanded to the torque motor, I_c , and took the form of a random input between -10A and 10A. Peak measured torques were $\sim 65Nm$. The commanded current and measured torque, τ_{meas} are shown in Fig. 5-a. The commanded joint torque, $\tau_c = I_cNK_t$, can be computed from the current command, the transmission ratio, N, and the motor torque constant, K_t . The torque control performance can be determined by comparing the measured torque, τ_{meas} , to τ_c . The measured frequency response is shown in Fig. 5-b. The 0.707 bandwidth was measured from the experimental results, and was 28Hz for unlubricated ropes (shown in Fig. 5-b) and 27Hz for lubricated ropes.

A simplified, linear lumped parameter model was fit to the data by tuning damping and stiffness parameters. Analysis of component properties implies that the bandwidth is limited by both the Vectran rope elasticity and the output shaft stiffness. The long active length of the cables $(\sim 0.45m)$ means that their

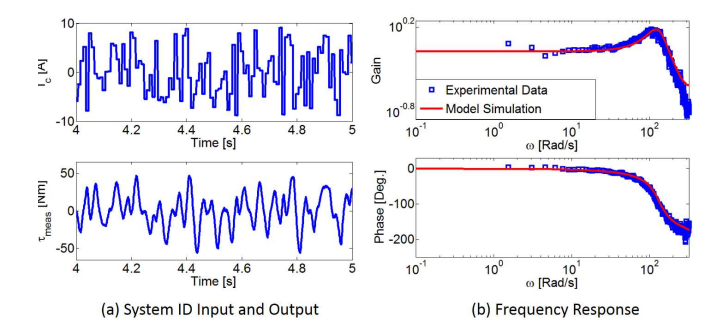


Fig. 5. Time series (a) and frequency response (b) for the system identification of the drive system.

stiffness affects the system dynamics. Other parts such as the load cell and couplings are estimated to be far stiffer than the rope. Angle data from the position motor also demonstrated a high stiffness, and removing the position motor dynamics did not significantly alter the results.

VI. EFFICIENCY

The efficiency of the synthetic rope drive system was estimated by using the torque motor to back-drive the un-powered position motor. The friction and inertia of the large position motor provide a substantial load to resist the torque motor. A sequence of positive and negative step current commands was used to emulate the cyclic and bidirectional nature of walking motions. These motions include regions with zero velocity and zero torque. Joint torque commands ranging from 16-32Nm in magnitude were used, corresponding to 19-66W of average mechanical power. Measurements were taken with unlubricated ropes and with ropes that had Krytox lubricant worked into the fibers.

To estimate the efficiency, we create a control volume encompassing the torque motor and transmission, shown in Fig. 6-a. The quantity E_1 represents the energy into the torque motor and is determined by measuring the voltages and currents into each of the 3 motor phases. The quantity E_2 represents the energy out of the drive system and is determined by measuring the torque and position at the output shaft. Energy is lost to resistive losses in the motor phases, E_R , and in the rope drive transmission, E_T . All other losses and any energy stored in the control volume are not modeled specifically and get lumped into our estimate of E_T . Conservation of energy for the control volume yields the following

$$E_1 - E_R - E_T - E_2 = 0 (6)$$

The efficiency of the motor and drive system, η_{sys} can be determined from E_1 and E_2 .

$$\eta_{sys} = \frac{E_2}{E_1} \tag{7}$$

The resistive loss, E_R , is highly dependent on torque. E_R represents Joule heating and is estimated from the measured current, I(t), and the measured motor phase-to-phase resistance, R_m . The transmission efficiency, η_T , can be estimated from E_2, E_1, E_R .

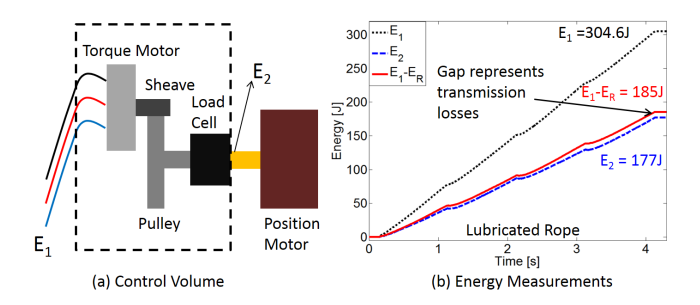


Fig. 6. Diagram of the test-stand control volume (a), and energy measurement data from the efficiency trajectory (b). The gap between the red and blue lines in the measured data is the energy lost in the drive system, E_T .

$$E_R = \int I(t)^2 R_m dt. \tag{8}$$

$$\eta_T = \frac{E_2}{E_1 - E_R} \tag{9}$$

Average estimates for the efficiency of the entire transmission system range are 0.95 for unlubricated ropes and 0.96 for lubricated ropes. Over the loads tested, transmission efficiency appears to increase slightly with load. One set of experimental results (27Nm command, 44W average mechanical power) is shown in Fig. 6-b.

A consequence of the high efficiency of the synthetic rope drive is its quiet operation. This is highlighted in the accompanying video. Sound pressure levels of the motor and transmission in motion were measured using a BAFX Advanced Sound Meter at a distance of 305mm. The measured sound pressure is roughly 60dBA— significantly quieter than normal conversation at this distance (70dBA).

VII. ENDURANCE

Rope endurance was characterized on the test-bed using time-synchronized motion and torque trajectories representative of simulated and real walking behaviors. Ropes were tensioned periodically during the first 1,000 cycles. A variety of trajectories and ropes were tested, and the results are summarized in Fig. 7. For simplicity, the various testing conditions are numbered 1-11, and are referred to as "RT's" ("rope tests"). In early development, a few terminations failed immediately under load, with the rope pulling free from the epoxy. These "infant termination failures" (RT1) indicate failures of quality control in termination fabrication.

A. Initial Testing: 3mm Vectran

Most RTs used 3mm V12 Vectran from New England ropes. A preliminary trajectory involving simple positive and negative 20Nm torque commands was first used to examine rope behavior. This trajectory reached the ends of the pulley, and the rope failed in this area after 20,000 cycles (RT2). A candidate trajectory was selected from walking simulations developed by the Florida Institute of Human and Machine Cognition (IHMC). The trajectory is from hip extension/flexion during fast walking and creates aggressive torque and speed conditions. Several variants were tested using this trajectory. Peak loads of 125Nm were initially used (RTs 3-5).

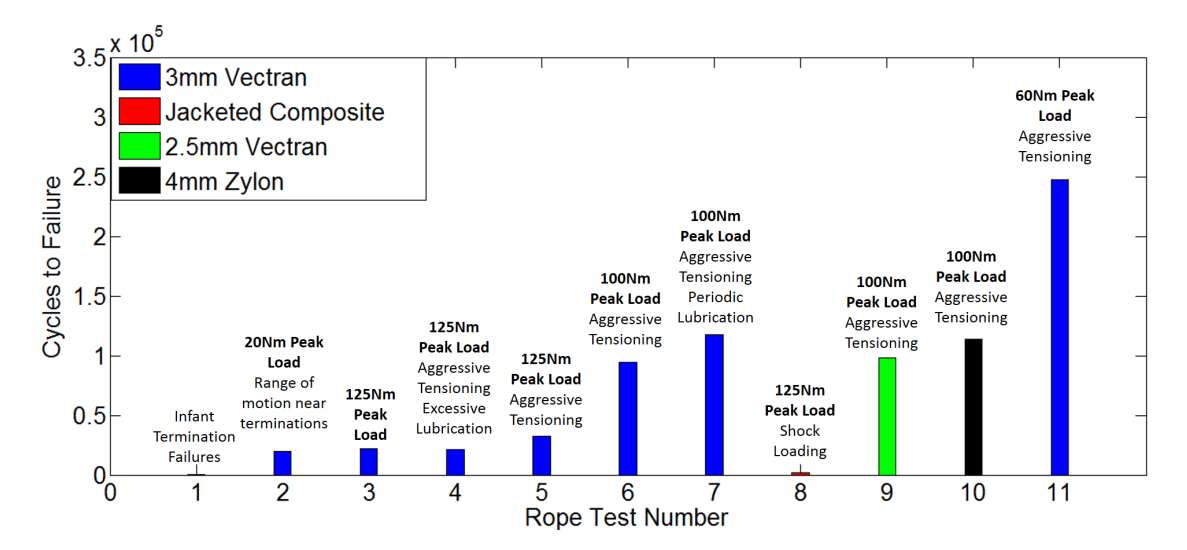


Fig. 7. A bar graph summarizing the rope endurance test results.

- 1) Role of Pre-Tensioning: Aggressive tensioning of the ropes was shown to extend life substantially by preventing shock due to load variations. Ropes were tightened until they did not slide on the pulley when pushed by hand. Life was extended from 22,000 cycles (RT3) to 32,500 cycles (RT5).
- 2) Role of Load: To examine load dependence, the peak load was reduced to 100Nm. This 20% reduction in load resulted in a nearly 3 fold increase in rope life, as can be seen by comparing RT5 and RT6.
- 3) Role of Proper Lubrication: The benefits and perils of lubrication were studied in RT4 and RT7. Krytox grease was applied to the ropes to reduce self-abrasion. In RT4, ropes were lubricated very near the terminations, reducing the capstan effect and transmitting large loads to the terminations. As a result, the rope failed at the termination after only 21,000 cycles. In contrast, RTs 2, 3, and 5-11 all failed away from the termination and near the location on the rope that bears the trajectory's peak torque. When applied only to the moving rope segments away from the terminations, lubricant can increase life by roughly 20%. The results of RT7 illustrate how periodic (every 7500 cycles) applications of lubricant added nearly 23,000 cycles to the rope life when compared with RT6.

B. Other Rope Types

Three additional rope types were tested without lubrication: a jacketed composite, 2.5mm diameter Vectran, and 4mm Zylon. With the jacketed composite, the jacket made properly tensioning the rope impossible. The rope visibly slackened during tests and failed after only 2,000 cycles (RT8). The 2.5mm Vectran from Samson ropes (RT9) was used to explore the role of a slightly smaller diameter. The rope survived 97,765 cycles, roughly the same as the unlubricated 3mm Vectran. RT10 used 4mm Zylon rope with the protective outer jacket removed. The Zylon rope survived 113,774 cycles, outperforming the unlubricated 3mm Vectran. However, Zylon has poor UV resistance: one study has shown that unsheathed Zylon loses more than 70% of its tensile strength after 144 hours of exposure to UV light [26]. Vectran can also have

low resistance to UV light, but can be treated with coatings to improve performance. Silicone oil treated (Vectran T97) loses only about 30% of its tenacity in the presence of UV light after 600 hours of exposure [12].

C. 3mm Vectran with Robot Trajectory

Projected rope life during robot walking was estimated using gait data obtained from our walking robots. These robots use several passive dynamic elements to reduce core drivetrain load at the joints, and therefore loads are considerably lower than the original design values [25]. The trajectory from one of the ankle joints featured the highest motor torques and was therefore selected for testing. This trajectory features 60Nm peak torques, and was tested using aggressive pretensioning (RT11) without lubrication. The 3mm Vectran rope survived 247,614 cycles which corresponds to roughly 150km of walking. This test is believed to be the most representative of typical loading on the WANDERER robot (Section IX).

VIII. COMPARISON WITH OTHER TRANSMISSION APPROACHES

Comparisons with other transmission types were performed using a notional 6:1 drive system rated to 150Nm. The output torque was chosen to roughly match the notional torque limit of our 6:1 rope drive which is currently limited by the strength of the terminations (Section IV). The other components and the ropes themselves are capable of transmitting up to 270Nm. As the rope terminations improve, the comparative mass and size savings from of our synthetic rope drive will increase.

A. Gears

Synthetic rope drives provide two advantages when compared with spur gears: backlash and mass. Cable based capstan drives have theoretically zero backlash [6], which is impossible with compact, low friction gearing. Sample gears were designed using the American Gear Manufacturers Standard (AGMA 220) for a 150Nm output torque [27]. Efforts were

made to ensure an accurate comparison by using only steel teeth on the output gear. The remainder of the output gear is aluminum. The combined mass of the input and output gears is 1.0kg. In contrast, the combined mass of the rope drive sheave, pulley, ropes, tensioning components, and terminations is 0.46kg. Similar analysis was performed for a 6:1 planetary gear design. The combined mass of the 3 planet gears, the ring gear, the sun gear, and the planet carrier is 1.2kg. Gears can also be susceptible to impacts with the environment [21]. We hypothesize that the rope elasticity would enhance the impact tolerance of the synthetic cable drive.

B. Harmonic Drive

Harmonic drives offer high efficiency, torque capacity, compact size, and zero backlash. However, harmonic drives are generally suitable for large reductions (30:1 to 320:1) [28]. In this work we desire much lower ratios (10:1). Achieving such low ratios with strain wave gearing is difficult. As the transmission ratio reduces, the teeth grow larger and greater deflections of the flex-spline are required [28]. Finite element techniques and optimization have been used to achieve ratios of 30:1, but this may represent a lower practical limit [28].

C. Steel Cable

Synthetic ropes provide an endurance/size advantage over steel cables. Steel cable manufacturers recommend a minimum ratio of curvature to rope diameter of 18:1 for 3.2mm, 7×19 , steel cables (versus 8:1 for braided Vectran) [9], [11]. Since the strength of steel cable and Vectran fiber is comparable, this means that proper usage requires an input sheave and output pulley that are 2.25 times larger when using steel cables. Violating the bend ratio recommendation can reduce endurance life to levels that are not practical. We illustrate this with a transmission using equivalent strength steel cable (3.2mm diameter) combined with the same-sized components as those for the Vectran fiber. This design is similar to the Vectran transmission described earlier: the gear ratio and package size are the same. However, in order to match size, the steel cable is subjected to an 8:1 bend radius on the sheave rather than the 18:1 it is designed for.

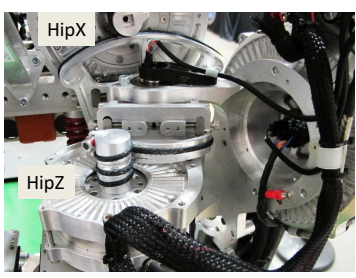
The performance of the steel-cable drive was evaluated on the test-bed. The steel cable drive is quiet, has good efficiency (0.95), and improved bandwidth (34Hz). Endurance was evaluated using the hip flexion/extension trajectory with a 100Nm peak torque. The steel cable drive failed after 3,381 cycles. When compared to the lifetimes demonstrated in Fig. 7, this steel cable has far lower endurance life than the Vectran.

D. Belt Drive

Synchronous belts offer high efficiency and negligible backlash. The size of components tends to be larger than those for synthetic rope drives, due to tensile strength limitations of the belt. Based on a 6:1 design with 150Nm output torque, the belt width is 40mm with high strength, steel-reinforced belts (5mm pitch). The belt width should not exceed the sheave diameter [27], so the belt sheave would be 40mm in diameter,



(a) Hip flexion/extension joint





(b) Compact integration of hip joints

Fig. 8. Photographs of the rope drive system on the WANDERER robot.

or 50% larger than the synthetic rope sheave. Synchronous belts also require continuous rotation, meaning that a full circle is required at the output. This increases the design footprint, especially for joints with small output motions.

IX. ROBOT INTEGRATION

We have incorporated these drive systems into two fullyactuated, 3D, human-scale, bipedal robots which use the synthetic rope transmissions at each of their 12 leg joints. Our latest prototype, the Walking Anthropomorphic Novelly Driven Efficient Robot for Emergency Response (WANDERER) is shown in Fig. 8. The transmission ratios range from 5 to 10, but are otherwise identical across joints. All leg joints use the same tensioning mechanism, 3mm Vectran ropes, and a 25.4mm diameter input sheave. Photographs of the rope drive systems incorporated into WANDERER are provided in Fig. 8-a,b. These photos illustrate the tensioning mechanism, and the compact nature of the drives. Fig. 8-a shows the hip flexion/extension joint (HipY), and Fig. 8-b shows how the compact nature of the synthetic rope drive enables effective packaging of the other two hip joints (x: ab/adduction, z: inversion/eversion).

To illustrate torque tracking performance, knee torque data during unsupported 3D walking was measured using a robot instrumented with strain gauges. The data shown in Fig. 9, illustrates how the measured torque, τ_m , tracks the commanded torque, τ_c , using current-only control. The accompanying video illustrates the performance of WANDERER. WANDERER was demonstrated at the Technology Exposition section of the 2015 DARPA Robotics Challenge Finals as part of the "Robot Endurance Test" where it walked 2.8km on one battery charge. To date, WANDERER has walked for 10-12 hours ($\sim 16,000$ cycles) without a rope failure.

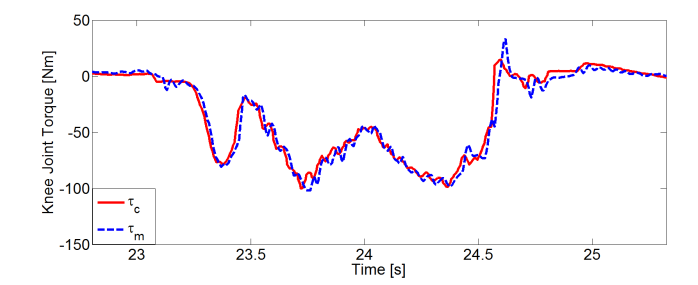


Fig. 9. Data illustrating torque tracking during bipedal walking.

X. CONCLUSIONS

This work demonstrates that capstan drives with synthetic ropes can provide impressive efficiency and torque control in a lightweight package. The potential issues with this approach stem mainly from rope elasticity and endurance. Despite the presence of rope elasticity, we achieved good torque control bandwidth (28Hz). However, the rope stretch under load (up to 0.1 radians at the output) means that many applications (e.g. our bipedal robots) require output position measurement. While knowledge of rope failure mechanics remains limited, our testing shows that with proper care, lifetimes of hundreds of thousands of cycles are achievable. This is competitive with prior reports of failures of steel and tungsten cables [8].

The specific synthetic rope drive system outlined in this work minimizes size and weight, eases assembly and rope tightening, and maximizes rope endurance. The experimental results illustrate that this drive system is capable of high bandwidth torque control, quiet operation, and efficient power transmission, while providing a record of the impact of lubrication, tensioning, and load on endurance. The rope drives have been shown to survive up to 247,000 cycles, and have demonstrated good performance during bipedal walking.

ACKNOWLEDGMENT

We thank Morgan Quigley at the Open Source Robotics Foundation for developing the motor power electronics, and we thank Gregory Brunson and Nadia Coleman for their contributions to testing. Finally, we thank Jerry Pratt, Peter Neuhaus, Sylvain Bertrand, Tingfan Wu, Jesper Smith, and Douglas Stephen at the Florida Institute for Human and Machine Cognition for their work on walking control.

REFERENCES

- J. Hollerbach, I. Hunter, and J. Ballantyne, A Comparative Analysis of Actuator Technologies for Robotics, The Robotics Review 2. Cambridge, MA: MIT Press. 1992.
- [2] A. Wang and S. Kim, "Directional Efficiency in Geared Transmissions: Characterization of Backdrivability Towards Improved Proprioceptive Control," in *Proc. of the 2015 IEEE International Conference on Robotics and Automation (ICRA 2015)*, Seattle, WA, May 2015, pp. 1055–1062.
- [3] W. Townsend and J. Guertin, "Teleoperator slave WAM design methodology," *Industrial Robot*, vol. 26, no. 167, 1999.
- [4] J. Grimes and J. Hurst, "The Design of ATRIAS 1.0 a Unique Monoped, Hopping Robot," in Proc. of the 2012 IEEE International Conference on Climbing and Walking Robots and Support Technologies for Mobile Machines, Baltimore, MD, 2012, pp. 548–554.

- [5] T. Massie and K. Salisbury, "The PHANTOM Haptic Interface: A Device for Probing Virtual Objects," in Proc. of the 1994 ASME Winter Annual Meeting: Symposium on Haptic Interfaces for Virtual Environment and Teleoperator Systems, November 1994, pp. 295–300.
- [6] J. Werkmeister and A. Slcoum, "Theoretical and experimental determination of capstan drive stiffness," *Precision Engineering*, vol. 31, pp. 55–67, 2007.
- [7] O. Baser and E. Konukseven, "Theoretical and experimental determination of capstan drive slip error," *Mechanism and Machine Theory*, vol. 45, pp. 815–827, 2010.
- [8] M. Summers, "Rope Selection for Rope Drive Transmissions Used in Robotic Manipulation," Bachelor's Thesis, Oregon State University, Corvallis, OR, 2010.
- [9] L. C. T. Library. (2015) Minimum Tread Diameter for Pulleys and Sheaves. Loos and Co. Pomfret, CT. [Online]. Available: http://www.loosco.com/resource-library/technicalinformation/pulley-sheave-diameters/
- [10] D. Beers and J. Ramirez, "Vectran high-performance Fibre," *The Journal of the Textile Institute*, vol. 81, no. 4, pp. 561–574, 1990.
- [11] S. Rope, "Rope user's manual: Guide to rope selection, handling, usage, and retirement," Samson Rope, Ferndale, WA, Tech. Rep., 2014.
- [12] K. America, "Vectran: Grasp the World of Toomorrow," Kuraray America, Fort Mill, SC, Tech. Rep., 2006.
- [13] S. Kitano, S. Hirose, A. Horigome et al., "TITAN-XIII: Sprawlingtype quadruped robot with ability of fast and energy-efficient walking," ROBOMECH Journal, vol. 3, no. 8, 2016.
- [14] L. Bridgewater, C. Ihrke, M. Diftler et al., "The Robonaut 2 Hand-Designed To Do Work With Tools," in Proc. of the 2012 IEEE International Conference on Robotics and Automation (ICRA 2012), Saint Paul, MN, May 2012, pp. 3425–3430.
- [15] J. Caputo and S. Collins, "An Experimental Robotic Testbed for Accelerated Development of Ankle Prostheses," in *Proc. of the 2013 IEEE International Conference on Robotics and Automation (ICRA 2013)*, Karlsruhe, DE, May 2013, pp. 2645–2650.
- [16] F. Sloan, S. Bull, and R. Longerich, "Design Modifications to Increase Fatigue Life of Fiber Ropes," in *Proc. of the 2005 IEEE/MTS OCEANS Conference (OCEANS 2005)*, Washington, DC, September 2005, pp. 829–835
- [17] N. Hogan, "Impedance Control: An Approach to Manipulation: Part I-Theory," ASME Journal of Dynamic Systems, Measurement, and Control, vol. 10, no. 1, pp. 1–7, 1985.
- [18] G. Kenneally, A. De, and D. Koditschek, "Design principles for a family of direct-drive legged robots," *IEEE Robotics and Automation Letters*, vol. 1, no. 2, pp. 900–907, 2016.
- [19] J. Colgate and N. Hogan, "Robust control of dynamically interacting systems," *International Journal of Control*, vol. 48, no. 1, pp. 65–88, 1088
- [20] S. Buerger and N. Hogan, Novel Actuation Methods for High force Haptics, Advances in Haptics. Rijeka, Croatia: InTech, 2010.
- [21] G. Pratt, "Low impedance walking robots," *Integrative and Comparative Biology*, vol. 42, pp. 174–181, 2002.
- [22] F. Faulhaber, "A Second Look at Gearbox Efficiencies," Machine Design, vol. 74, pp. 82–84, 2002.
- [23] S. Seok, A. Wang, M. Chuah et al., "Design Principles for Energy-Efficient Legged Locomotion and Implementation on the MIT Cheetah Robot," *IEEE/ASME Transactions on Mechatronics*, vol. 20, no. 3, pp. 1117–1129, 2015.
- [24] A. Horigome and G. Endo, "Basic study for drive mechanism with synthetic fiber rope- investigation of strength reduction by bending and terminal fixation method," *Advanced Robotics*, vol. 30, no. 3, pp. 206– 217, 2016.
- [25] A. Mazumdar, S. Spencer, J. Salton et al., "Using Parallel Stiffness to Achieve Improved Locomotive Efficiency with the Sandia STEPPR Robot," in Proc. of the 2015 IEEE International Conference on Robotics and Automation (ICRA 2015), Seattle, WA, May 2015, pp. 835–841.
- [26] J. Won, M. Said, and A. Seyam, "Development of UV protective sheath for high performance fibers for high altitude applications," *Fibers and Polymers*, vol. 14, no. 4, pp. 647–652, 2013.
- [27] E. Oberg, F. Jones, H. Horton et al., Machinery's Handbook. New York: Industrial Press, 2004.
- [28] K. Ueura and R. Slatter, "ACTUATORS: Development of the harmonic drive gear for space applications," in *Proc. of the 8th European Sympo*sium on Space Mechanisms and Tribology), Toulouse, Fr, October 1999, pp. 829–835.